Check for updates

Electrochemical Science Advances

WILEY-VCH

ELECTROCHEMICAL SCIENCE ADVANCES Open Access

PERSPECTIVE OPEN ACCESS

Technological Advances in the Electroreduction of CO_2 to HCOOH: The Impact of Catalyst, Gas Diffusion Electrode, and Cell Design

Verena Theußl[1,2,‡] | Sergio Sanz[1,‡] | Konstantin von Foerster[1,2,‡] | Bastian Rutjens[1,2] | Henning Weinrich[1] | Hermann Tempel[1] | Rüdiger-A. Eichel[1,2]

[1]Institute of Energy Technologies – Fundamental Electrochemistry (IET-1), Forschungszentrum Jülich, Jülich, Germany | [2]RWTH Aachen University, Institute of Physical Chemistry, Aachen, Germany

Correspondence: Verena Theußl (v.theussl@fz-juelich.de)

Received: 10 June 2024 | **Revised:** 15 September 2024 | **Accepted:** 7 October 2024

Funding: This study was funded by Bundesministerium für Bildung und Forschung 3SF0627A.

Keywords: Catalyst | CO_2 reduction | Electrocatalysis | Electrolyzer | Formic acid | Gas Diffusion Electrode

ABSTRACT

The electrochemical reduction of carbon dioxide (eCO_2RR) is a promising technology for synthesizing value-added products required in the transition towards a more circular and renewable-based economy. In this context, the electrochemical production of formic acid has the potential to become economically competitive to energy-demanding conventional synthetic methods, thereby presenting a sustainable alternative. However, to enhance energy efficiency and selectivity toward the targeted product significant technological improvements in key components (e.g., electrodes, catalysts, electrolytes, membranes, cells, solvents) are required. Over recent years, our research has focused on understanding the influence of catalyst, gas diffusion electrode (GDE) architecture and performance, and cell design in the eCO_2RR to formic acid. This perspective article provides an overview of the current status of these specific components, as well as our insights and those of other researchers, regarding potential future investigations and applications.

1 | Introduction

To achieve sustainability in industrial key sectors, it is necessary to re-structure processes to achieve the transition to a circular carbon economy [1, 2]. The electrochemical CO_2 reduction reaction (eCO_2RR) to formic acid (HCOOH) or formate ($HCOO^-$) helps in this endeavor by reducing the atmospheric concentration of CO_2 and represents an alternative to the energy-intensive industrial approach to this chemical, which requires the use of high pressure, temperature, and base.[3] The conventional industrial route to synthesized formic acid starts from methanol—carbonylation of methanol to produce methyl formate, followed by hydrolysis.[4] Hence, technological improvements within CO_2-to-HCOOH electrolysis, with the possibility to couple them to renewable sources such as wind and solar power are paramount to enable this CO_2-negative synthetic transformation.[5] Herein, the term Power-to-HCOOH comes into play as a promising approach to convert electrical power, especially that generated from renewable sources during periods of high availability, into HCOOH as a storage fuel and chemical.[6] This could be converted back into energy during periods of low renewable energy production. Besides, the current

Correction added on 25 November 2024, after first online publication: the affiliations of the fourth author have been updated.

‡V. Theußl, S. Sanz, and K. v. Foerster contributed equally to this work.

This is an open access article under the terms of the Creative Commons Attribution License, which permits use, distribution and reproduction in any medium, provided the original work is properly cited.

© 2024 The Author(s). *Electrochemical Science Advances* published by Wiley-VCH GmbH.

concentrations of CO_2 in the atmosphere, along with future predictions, necessitate the exploration of technologies such as CO_2 capture and storage to effectively mitigate the effects of climate change [7–9]. CO_2 electroreduction benefits from these technologies, as it guarantees renewable feed supply. HCOOH offers a valorization option in various fields, such as the textile and leather industries, as a preservative and antibacterial agent, in the rubber industry, as a pH regulator for food products, and in biological and medical research. Other potential applications, still under investigation, include its use as an energy carrier for global transportation logistics and application in direct formic acid fuel cells, indirect formic acid fuel cells, syngas storage medium, chemical reagent in organic synthesis (e.g., as CO surrogate), and feed for bioprocesses [4, 10]. Compared to other eCO_2RR products, HCOOH has the potential to become economically competitive with conventional synthesis routes.[11, 12] However, its implementation still requires improvements in energy efficiency, current density, selectivity, and operation time. In this regard, technological advances are paramount toward enhanced product selectivity at higher current density. We, among other researchers, have a great interest in understanding, within the eCO_2RR to HCOOH, the effect of catalyst, gas diffusion electrode (GDE) architecture and performance, and cell design. Hence, this article showcases our thoughts in combination with those of other groups on these key points.

1.1 | Electrocatalysts

Most of the research within eCO_2RR has focused on C_1 products, where the $2e^-$ reactions yielding CO and HCOOH are the most favorable. Although the electroreduction to other hydrocarbon or alcohol products is thermodynamically more favorable by their standard potentials, the requirement for more electron equivalents renders them kinetically less favorable.[13, 14] In the context of HCOOH production, operating within the potential range for the eCO_2RR to HCOOH inevitably results in some degree of hydrogen evolution reaction (HER) and CO production. Hence, kinetic differentiation provided by catalyst selection is of utmost importance for achieving the targeted product with high selectivity and efficiency [15, 16]. This underscores the necessity for a deep understanding of the reaction mechanism, which is essential for advancing in the field toward more sustainable and efficient chemical transformations [17]. The lack of experimental observations, given the heterogeneity of the catalysis and operational setup, makes it difficult to monitor the reaction and isolation of intermediates. Therefore, the elucidation of the catalytic mechanism relies heavily on computational studies. These propose three possible mechanisms (Figure 1a), in which HCOOH evolving from an *OCOH intermediate (* denotes the surface site binding to the adjacent atom, i.e., oxygen) is the most energetically favorable (Figure 1c).[17–20] Unlike other C_1 products (CO, methane, methanol), which are suggested to develop through the initial *COOH and subsequent *CO species, the reduction of CO_2 to HCOOH follows a distinct route [21].

Catalysts based on tin, bismuth, indium, lead, palladium, and cobalt elements have been tested and are promising candidates in the eCO_2RR to HCOOH (see also Table 1) [22–25]. Tin and bismuth exhibit both high activity and selectivity and are widely abundant and environmentally friendly [3, 5, 26]. Additionally, compared to metals with high market prices (e.g., indium, palladium), toxicity (lead), and low selectivity (e.g., cobalt), tin- and bismuth-based catalysts emerge as a popular choice in the scientific community. The literature is dominated by tin and tin alloys, where the production of HCOOH can be enhanced by engineering defects or doping to modulate the reactions at the catalyst surface. In the last years, the development of synthetic methods to produce high surface areas possessing many active sites focused on metal-oxide and metal-sulfide has attracted a lot of attention. Studies on bismuth oxides demonstrated that the selectivity of the high surface area of bismuth nanosheets outperformed that of bulk bismuth [27]. Our investigations with custom-made tin oxide catalysts also showed that the presence of high surface area accounts for better performances. We produced tin oxide nanoparticles by hydrothermal (~5 nm), sol-gel (> 10 nm), and solid-state (10–20 nm) synthetic procedures (Figure 2b–d). The best performance in terms of Faradaic efficiency was obtained with the hydrothermal particles, which we ascribed to the large surface area and a large number of lattice defects [28]. The conversion of CO_2 to HCOOH, as for other eCO_2RR products, is limited by the low solubility of CO_2 in aqueous electrolytes. The use of GDEs circumvents this problem and allows selectively producing HCOOH at higher current densities. Deposits of tin oxides and tin on GDEs achieved current densities of 385 ± 19 and 214 ± 6 mA cm^{-2} respectively, with $HCOO^-$ selectivity > 70% [29]. *In operando* ATR-IR spectroscopy indicated the presence of a tin carbonate intermediate and helped in the proposal of a new mechanism (Figure 2a). A two-electron reduction converts SnO_2 to Sn^{II} oxyhydroxide, which reacts with CO_2 to form Sn-OCOOH. Subsequently, through a two-electron proton-coupled reaction, the Sn^{II} oxyhydroxide is restored, with the release of $HCOO^-$.[30] Based on this knowledge, a two-valence tin oxide nanosheet grown on nanorods producing 94% of $HCOO^-$ at ~330 mA cm^{-2} was developed [31]. The authors attributed this high efficiency to the presence of abundant low coordination Sn^{II} active sites.

Despite current advancements in catalysis design, the search for active and selective electrocatalysts with low cost still remains a challenge to activate the kinetically sluggish CO_2 reduction reaction—especially when aimed for large-scale production—emphasizing the need for a better understanding of the reaction mechanisms.

1.2 | Gas Diffusion Electrodes

In the last decades, the research in the field of CO_2 electroreduction mainly focused on the synthesis of active and selective catalysts. However, the classical cell setups commonly employed to investigate these materials are constrained by the low diffusion coefficient of the dissolved CO_2 in the bulk electrolyte [50] together with the long diffusion distance to the electrode. These factors hinder the sufficient availability of CO_2 on the catalyst surface, leading not only to a CO_2-starved catalyst layer but also resulting in a favored parasitic HER as a side reaction. Furthermore, it restricts the achievable current densities to a few mA cm^{-2},[51] which considerably lags behind the high current densities (> 300 mA cm^{-2}) necessary for industrial application.[52] To overcome these diffusion and mass transport limitations GDE can be used due to its unique structure.[53] GDEs enable the direct feeding of the CO_2 gas to

26985977, 0, Downloaded from https://chemistry-europe.onlinelibrary.wiley.com/doi/10.1002/elsa.202400014 by Rwth Aachen University Universitätsbibliothek- 021000, Wiley Online Library on [10/01/2025]. See the Terms and Conditions (https://onlinelibrary.wiley.com/terms-and-conditions) on Wiley Online Library for rules of use; OA articles are governed by the applicable Creative Commons License

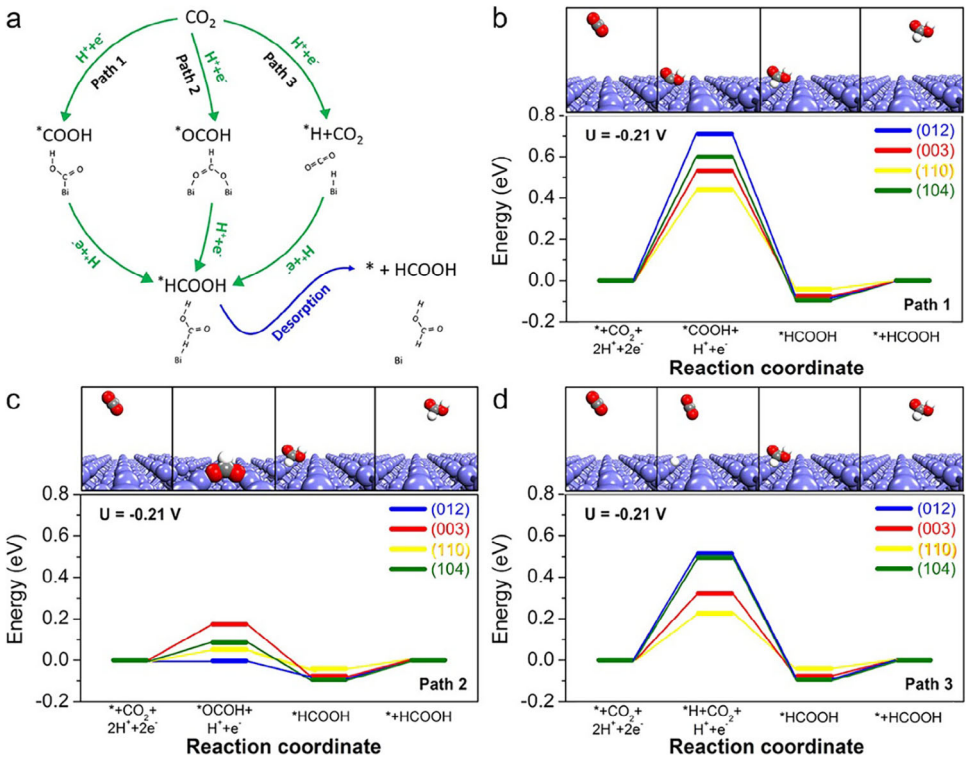

FIGURE 1 | DFT calculations on the different reaction pathways for the eCO_2RR to HCOOH on bismuth planes of (012), (003), (110), and (104). (a) Scheme of the three possible mechanism paths, which proceed via a *COOH intermediate (path 1), *OCOH intermediate (path 2), or the formation of *H (path 3). Reaction free energy diagrams for (b) path 1, (c) path 2, and (d) path 3, when zero overpotential is applied (bias potential U = –0.21 V_{SHE}). Reprinted with permission from ACS Catal. **2017**, 7, 5071–5077. Copyright 2017 American Chemical Society.

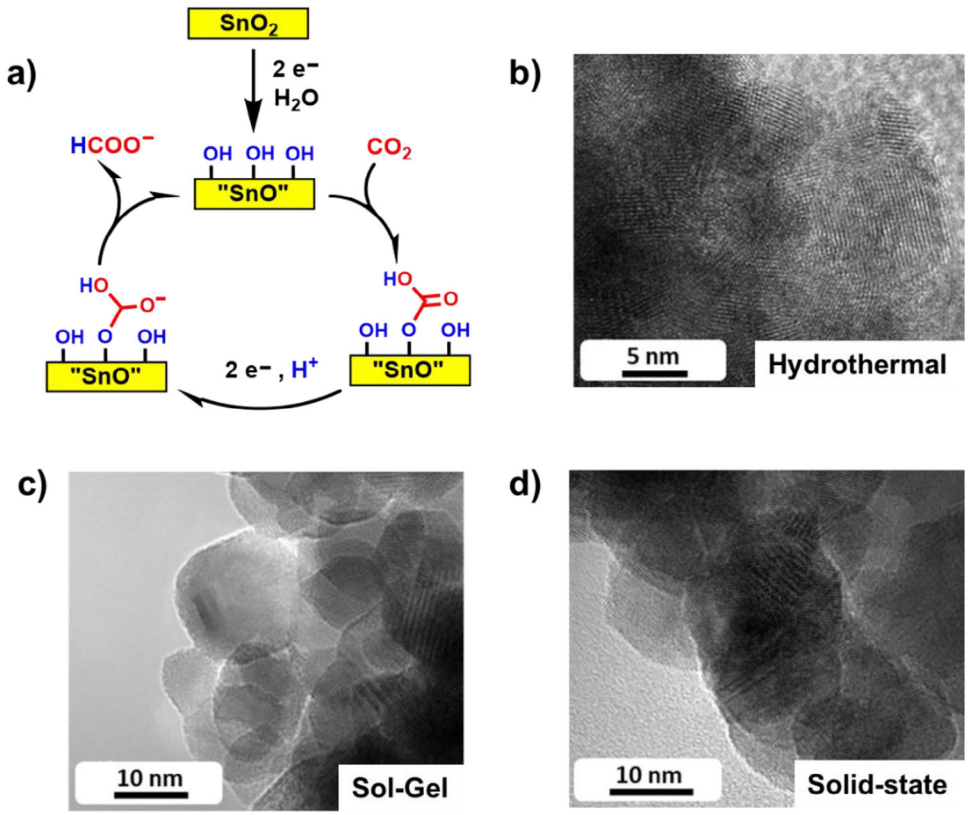

FIGURE 2 | (a) Possible reaction mechanism for the eCO_2RR to HCOO— on SnO_2 mediated by a surface-bound carbonate intermediate. TEM images of investigated SnO_2 nanoparticles at high magnification synthesized by (b) hydrothermal, (c) sol-gel, and (d) solid-state.

26985977, 0, Downloaded from https://chemistry-europe.onlinelibrary.wiley.com/doi/10.1002/ebsa.202400014 by Rwth Aachen University Universitätsbibliothek- 021000, Wiley Online Library on [10/01/2025]. See the Terms and Conditions (https://onlinelibrary.wiley.com/terms-and-conditions) on Wiley Online Library for rules of use; OA articles are governed by the applicable Creative Commons License

TABLE 1 | Representative examples of electrocatalysts active in the eCO_2RR to formic acid/formate. Examples of active electrocatalysts used in the different flow cell electrolyzers are displayed in Tables 2 and 3.

Electrocatalyst	Electrolyte	Applied potential/ [V]	Membrane	Anode	RE	Faradaic efficiency	Current density / [mA·cm [2]]	Ref.
SnO_2/graphene	0.1 M $NaHCO_3$	−1.80 (vs SCE)	Not given	Pt wire	SCE	94%	10.2	[32]
SnO_2 nanowires	0.1 M $KHCO_3$	−1.0 (vs RHE)	Selemion AMV (AEM)	Pt mesh	Ag/AgCl	80%	10	[33]
SnO_2 quantum wires	0.1 M $KHCO_3$	−1.25 (vs RHE)	Nafion N-117	Pt gauze	SCE	90%	18.1	[34]
SnO_2	0.5 M $KHCO_3$	−0.8 (vs RHE)	Nafion N-117	Pt gauze	SCE	80%	10	[35]
Bi nanoflakes	0.1 M $KHCO_3$	−0.6 (vs RHE)	Nafion	Pt mesh	Ag/AgCl	100%	5	[36]
Bi/BiOCl	0.5 M $KHCO_3$	−1.5 (vs SCE)	Nafion N-117	Pt plate	SCE	92%	3.7	[27]
Bi_2O_3	0.5 M $KHCO_3$	−0.9 (vs RHE)	Nafion N-117	Pt mesh	Ag/AgCl	91%	8	[37]
Bi_2O_3 nanoparticles	0.5 M $NaHCO_3$	−1.2 (vs RHE)	Nafion N-117	Pt foil	Ag/AgCl	91%	22	[38]
Bismuthene	0.5 M $NaHCO_3$	−0.58 (vs RHE)	Nafion N-117	Pt wire	SCE	98%	~ 3	[39]
In_2O_3/rGO	0.1 M $KHCO_3$	−1.2 (vs RHE)	Nafion N-115	Pt wire	Ag/AgCl	75%	22.5	[40]
In_2O_3/@C	0.5 M $KHCO_3$	−0.9 (vs RHE)	Nafion N-117	Pt plate	Ag/AgCl	87%	15	[41]
Pb-amine modified	1 M $KHCO_3$	−1.09 (vs RHE)	Nafion N-117	Pt gauze	SCE	94%	9.5	[42]
Pb nanoparticles/C nanotubes	0.5 M $KHCO_3$	−1.7 (vs RHE)	Nafion N-117	Pt	Ag/AgCl	84%	28	[43]
Pd nanoparticles	0.5 M $KHCO_3$	−0.2 (vs RHE)	Nafion N-117	Pt gauze	Ag/AgCl	90%	15	[44]
Pd-B/C	0.1 M $KHCO_3$	−0.5 (vs RHE)	Nafion N-117	Pt foil	SCE	70%	~ 10	[45]
Pd/C	2.8 M $KHCO_3$	−0.25 (vs RHE)	Selemion (AEM)	Pt foil	Ag/AgCl	~ 90%	~ 3	[46]
Co_3O_4 layers	0.1 M $KHCO_3$	−0.88 (vs SCE)	N/A (three-electrode system)	Graphite rod	SCE	64%	0.68	[47]
Co layers—partially oxidized	0.1 M Na_2SO_4	−0.85 (vs RHE)	N/A (three-electrode system)	Pt gauze	SCE	90%	10.59	[48]
Co_3O_4–oxygen vacancies	0.1 M $KHCO_3$	−0.87 (vs SCE)	N/A (three-electrode system)	Graphite rod	SCE	85%	2.7	[49]

26985977, 0, Downloaded from https://chemistry-europe.onlinelibrary.wiley.com/doi/10.1002/elsa.202400014 by Rwth Aachen University, Universitätsbibliothek, 021000, Wiley Online Library on [10/01/2025]. See the Terms and Conditions (https://onlinelibrary.wiley.com/terms-and-conditions) on Wiley Online Library for rules of use; OA articles are governed by the applicable Creative Commons License

the catalyst layer, facilitating reactant transport and distribution while enhancing the eCO_2RR through their unique multilayer configuration.[51] The first two layers of a GDE are called gas diffusion layer (GDL), and it is only when the catalyst is added on top that it becomes a complete GDE. The material of a GDL can consist not only of carbonaceous materials [54–56] but also of metals [57] (more specific to fuel cells) or polytetrafluoroethylene (PTFE).[58] In carbonaceous-based GDE,[53, 59–61] the multilayer structure consists of: i) the carbon fibers, ii) an optional microporous layer (MPL), and most importantly, iii) the catalyst layer. Across the different GDE layers PTFE is commonly employed for hydrophobic treatment to prevent early electrode flooding. The loss of hydrophobicity and/or binder degradation during operation, especially in flow electrolyzers, are the primary mechanisms triggering a decline in electrochemical performance due to electrode flooding [54, 62–67]. Other factors contributing to electrode deactivation include carbonate formation [68–70], catalyst agglomeration, and chemical changes including catalyst poisoning.[71, 72] Therefore, the investigation of gas diffusion electrodes is one important task in the implementation of the CO_2 electroreduction to HCOOH as it not only bears the catalyst layer but promotes the whole reduction reaction.

Among the different components of the multilayer structure of a carbonaceous-based GDE, the importance of a MPL is particularly notable. In a recent study, we observed how the presence of a MPL enhances both the cathodic current density at $-1.15\ V_{RHE}$ during linear sweep voltammetry (LSV) and the Faradaic efficiency compared to GDEs without one [53]. Our findings revealed that the MPL acts as a physical barrier for the nanoparticles during deposition, leading to a focused catalyst layer on top of the GDE and an enhanced contact to the electrolyte (Figure 3a). The open structure of the GDEs without MPL, however, leads to a deep penetration of the catalyst nanoparticles into the inner GDL volume. As a result, some catalyst nanoparticles are positioned beyond the reach of the electrolyte (Figure 3b), leading to lower Faradaic efficiency.[55, 73, 74] The hydrophobic treatment also plays a pivotal role in terms of obtained Faradaic efficiency, since the electrode wetting determines the extent of the CO_2 electroreduction at the GDE/electrolyte interface [75]. Recently [53], we showed that lower hydrophobic treatment (10% vs. 30%) at GDEs without MPL exhibited higher Faradaic efficiency. The degradation of the binder also influences changes in hydrophobicity. Throughout repeated operation of GDEs utilizing Nafion as a binder, we observed a decrease in Faradaic efficiency and a reduction in electrode potential, fostering the unwanted HER.[59] These effects likely stemmed from a progressive loss of hydrophobicity due to structural changes of the side chains and/or sulfonic groups, and states a rather unsuitability of Nafion as binder in the investigated setup. Considering our measurements were conducted in a gas-fed batch cell, comparing the impact of hydrophobic treatment to other designs, such as membrane electrode assemblies (MEA), might yield different results. We found reports indicating either superior performance in GDEs with higher PTFE content [76], or no significant impact of the hydrophobic treatment on the Faradaic efficiency.[55] Deactivating factors in the GDE, such as electrode flooding induced by the loss of hydrophobicity or thinning of the binder (Figure 3d), catalyst agglomeration (Figure 3e), carbonate formation (Figure 3f), and chemical changes (Figure 3g), directly affect the eCO_2RR efficiency. Hence, a meticulous GDE design, with minimal structural changes, particularly over extended operation times, is fundamental to guarantee high and stable HCOOH yields [71, 72, 77].

1.3 | Electrolysis Cells

To achieve industrial applicability, the eCO_2RR to HCOOH must be performed at high selectivity, high current density, low overall cell voltages, and with long-term stability [78]. A multitude of promising reactors have been designed for this purpose, including several designs of flow cells, such as zero-gap, anion exchange membrane (AEM) free, and direct formic acid production (DFAP) cell designs (Figures 4a–d).[79–87] In the context of this article, we do not consider other designs, particularly those with liquid-fed cathodes [88, 89], as they typically only enable low current densities. In the electrolyzers discussed here, the anode typically performs an oxygen evolution reaction (OER) in an aqueous anolyte and is separated from the cathode by at least a cation exchange membrane (CEM) or a bipolar membrane to avoid HCOO(H) loss at the anode. Each reactor design optimizes single performance indicators, albeit at the expense of others. Zero-gap reactors (Figure 4a) provide the lowest cell voltages and specific energy consumptions using OER in the anode (2.4 V and 3.35 $kWh \cdot kg^{-1}$ at 400 $mA \cdot cm^{-2}$) [90], while AEM-free cells (Figure 4b) can deliver the highest Faradaic efficiencies (100%) [86] and current densities (2000 $mA \cdot cm^{-2}$).[91] A three-compartment design, employing the hydrogen oxidation reaction (HOR) at the anode (Figure 4c) stands out for its capability to achieve the highest product concentrations (100%).[79] Tables 2 and 3 present the optimized performance indicators for each electrolyzer design. The majority of designs (Figures 4a, b, and d) involve the collection of HCOO(H) as a diluted product in water.[3, 4, 6, 10–12] Those employing alkaline electrolytes, such as KOH and $KHCO_3$, to mitigate the HER (Figures 4a, b) [4, 53, 80, 92–95] result in the formation of $HCOO^-$, necessitating energy-intensive workup to obtain HCOOH [52, 96]. While the use of acidic electrolytes such as H_2SO_4 and KCl nominally produce HCOOH [97, 98] in designs different from DFAP [99], the solution is saturated with alkaline salts required to suppress the HER.[98, 100]

In our investigations, we decided to utilize DFAP (Figure 4d) due to its capability of producing aqueous HCOOH free of electrolyte impurities [25] by using only distilled water as a liquid feed. Additionally, it offers performance advantages attributed to its specific design features, which include: (i) a gas-fed GDE cathode, facilitating high current densities, (ii) an anode fed with deionized water to avoid the presence of alkaline ions, (iii) a center compartment filled with a fixed bed of a proton exchange resin (for example Amberlite IR-120H) [99] to enhance proton conduction and provide structural stability, from which the protonated HCOOH product is flushed out using deionized water, (iv) a CEM situated between the anode and the center compartment, conducting protons while preventing HCOOH diffusion to the anode, and (v) an AEM positioned between the cathode and the center compartment, allowing the transport of $HCOO^-$ and OH^- anions, while maintaining alkalinity in the cathode by preventing back diffusion of HCOOH from the acidic center compartment to the alkaline cathode. Besides, the

26965977, 0, Downloaded from https://chemistry-europe.onlinelibrary.wiley.com/doi/10.1002/ebsa.202400014 by Rwth Aachen University Universitätsbibliothek - 021000, Wiley Online Library on [10/01/2025]. See the Terms and Conditions (https://onlinelibrary.wiley.com/terms-and-conditions) on Wiley Online Library for rules of use; OA articles are governed by the applicable Creative Commons License

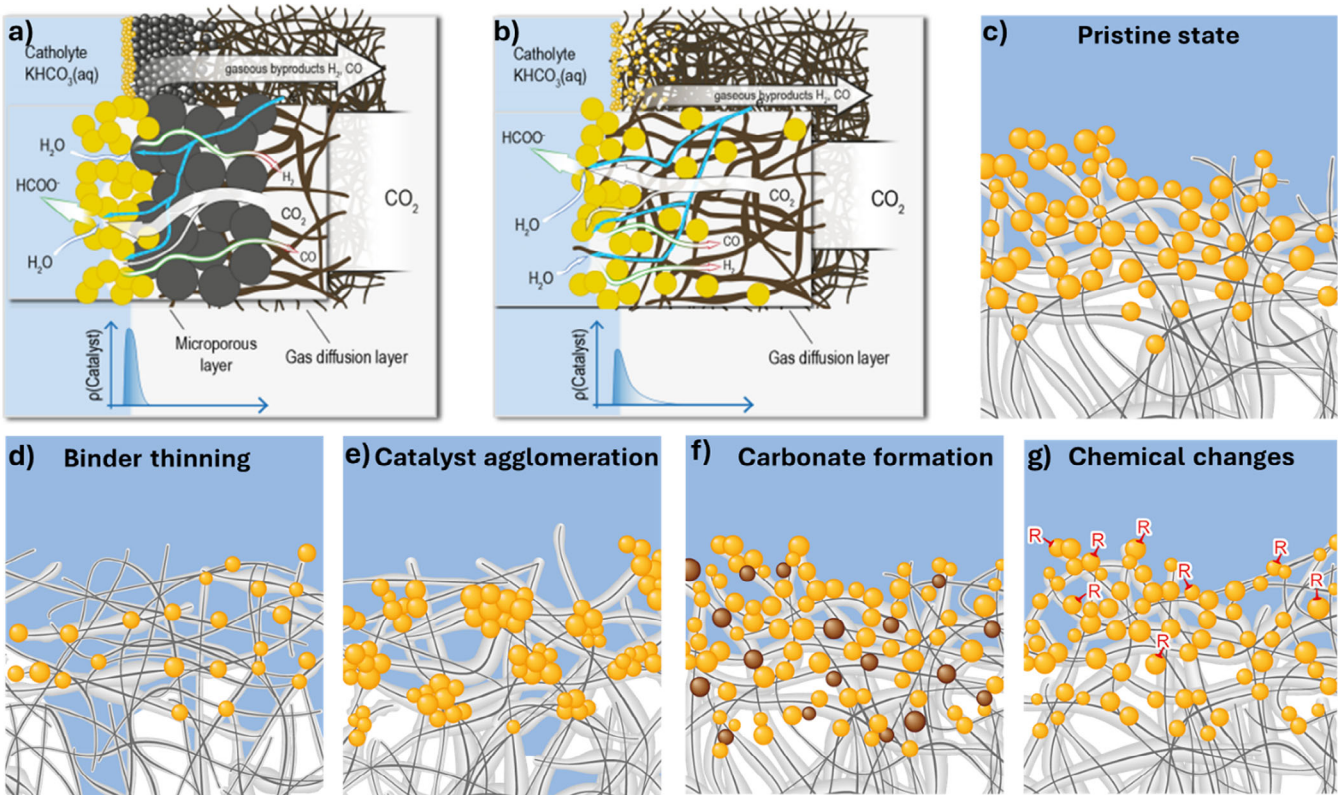

FIGURE 3 | Schematic illustration of the reaction conditions at the investigated gas diffusion electrodes (GDEs) surface, displaying an enlarged depiction as an inset. (a) GDE with a microporous layer (MPL) that leads to a focused catalyst layer on the GDE surface. (b) GDE without MPL, thus, missing physical barrier for the catalyst nanoparticles (SnO_2, shown in yellow color) during the GDE manufacturing. Representation of structural changes on the GDE during operation. (c) Pristine GDE state at t = 0, and final states showcasing deterioration by (d) binder thinning, (e) catalyst agglomeration, (f) carbonate formation—depicted in brown color, and (g) chemical changes occurring at the catalyst.

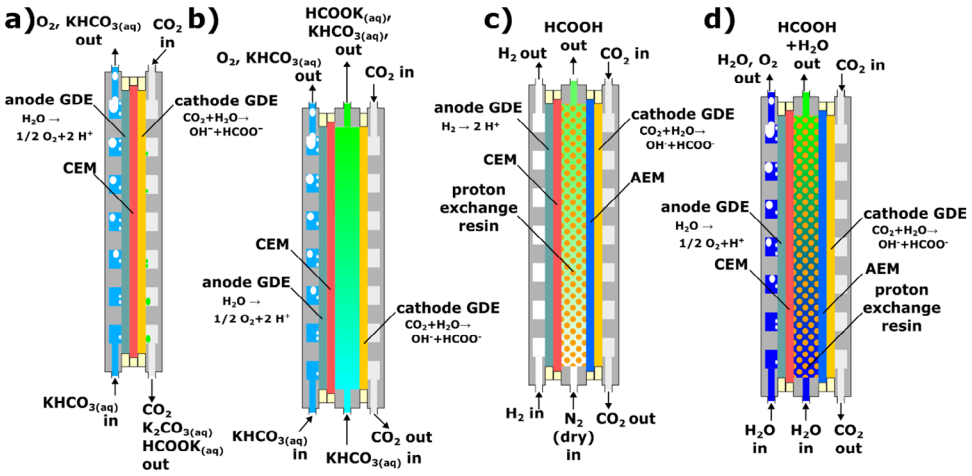

FIGURE 4 | Examples of CO_2-to-HCOO(H) reactor designs. a) Zero-gap, b) AEM-free c) gas-fed DFAP and d) water-fed DFAP cells.

AEM serves to regulate water transport to the cathode, hence, preventing its flooding and, as a consequence, the HER [81].

In DFAP, the production of a pure aqueous HCOOH solution eliminates concerns regarding salt precipitation due to the absence of alkaline ions and avoids post-treatment processes such as electrodialysis which simplifies product workup significantly. This makes DFAP arguably the most promising reactor design from an economic point of view [52, 96]. While the HOR-based DFAP (Figure 4c) requires H_2 as an expensive feed, the DFAP employing anodic OER requires only CO_2 and water as reactants, thereby reducing operational costs. This design offers enhanced performance indicators, including current densities of 250 mA cm^{-2} [99], cell voltages of 3.2 V [81], concentrations of 13wt% [99] (100% for short periods via an adapted design) [79], specific energy consumptions of 5.4 kWh kg^{-1}, and long-term

26985977, 0, Downloaded from https://chemistry-europe.onlinelibrary.wiley.com/doi/10.1002/elsa.202400014 by Rwth Aachen University Universitätsbibliothek- 021000, Wiley Online Library on [10/01/2025]. See the Terms and Conditions (https://onlinelibrary.wiley.com/terms-and-conditions) on Wiley Online Library for rules of use; OA articles are governed by the applicable Creative Commons License

TABLE 2 | Comparative overview of some performance indicators and GDE composition of representative examples in the eCO_2RR to formic acid/formate using zero gap and AEM-free electrolyzers.

Electrolyzer	Zero Gap	AEM free				
Cathode (Catalyst, Binder, GDL, active surface area)	MIL-68(In)-NH_2 Nafion Carbon GDL	Sn NP Nafion Sigracet 39 BC 16 cm^2	Sn Nafion TGP-H-060 25 cm^2	SnO_2 Nafion Sigracet 39 BC 1 cm^2	Sn plate	Bi/C NP Nafion TGP-H-60 (Vulcan XC72, PTFE) 10 cm^2
Membrane	FAB-PK-130	Nafion 117	Nafion 115	Selemion AMV AGC Inc.	Nafion 117	Nafion 117
Electrolyte	1 M $KHCO_3$	2 M KOH	1 M KOH	1 M KOH	0.5 M $KHCO_3$ + 0.6 M Na_2SO_4	0.45 M $KHCO_3$ + 0.5 M KCl / 1 M KOH
Anode	Pt sheet	Ni foam	Pt black	IrO_2 GDE	DSA	Ir MMO on Pt
Faradaic Efficiency / [%]	92.2	80	93.3	94	70	80
Current Density / [mA·cm^{-2}]	800	100		471	10	45
Energy Consumption / [kWh/kmol]	—	3.88	—	—	216	184
Concentration / [g/L]	—	65.4	41.5	—	0.46	200
Ref.	[114]	[115]	[116]	[117]	[118]	[119]

TABLE 3 | Comparative overview of some performance indicators and GDE composition of representative examples in the eCO_2RR to formic acid/formate using the DFAP electrolyzer setup.

Electrolyzer	DFAP with HOR	DFAP (zero gap with HOR)	DFAP with OER		
Cathode (Catalyst, Binder, GDL, active surface area)	Bi no binder Sigracet 35 BC 4.75	Bi_2O_3 AP1-CNN8-00-X Sigracet 39 BB 25	Bi_2O_3 Nafion YLS-30T 1	Sn NP Sustainion Carbon nanotubes TGP-H-120	SnBi Nafion+SiC PTFE fibers 2.89
Membrane	Sustainion/Nafion	PiperION-TP80-HCO3	Sustainion-x37-50 grade 60/Nafion 117	Sustainion Nafion 234	Sustainion-x37-FA/ Nafion 117
Electrolyte	none (CO_2/N_2/N_2 either dry or humid)	1 M KOH/DI H_2O	DI H_2O/DI H_2O	DI water	DI H_2O/0.5 M H_2SO_4
Anode	IrO_2/C GDE	Pt/C (HOR) on Nafion D2020	IrO_2 GDE	IrO_2 on expanded Ti	Pt foil
Faradaic Efficiency / [%]	52–94	35–75	68–84	94	39–91
Current Density / [mA·cm^{-2}]	10–840	25–500	14–86	140	10–250
Energy Consumption / [kWh/kmol]	39–110 (with HOR)	68–86 (with HOR)	105–145	—	124–247
Concentration / [g/L]	115–1150	3.7–12	4.6	94	19
Ref.	[79]	[90]	[120]	[81]	[98]

26985977, 0, Downloaded from https://chemistry-europe.onlinelibrary.wiley.com/doi/10.1002/ela.202400014 by Rwth Aachen University, Universitätsbibliothek- 02100, Wiley Online Library on [10/01/2025]. See the Terms and Conditions (https://onlinelibrary.wiley.com/terms-and-conditions) on Wiley Online Library for rules of use; OA articles are governed by the applicable Creative Commons License

operation exceeding 1000 h [99], making it a promising choice compared to other designs. But, while this significant progress has been made in understanding and optimizing this electrolyzer, the investigation of the AEM has been uniquely centered on the use of Sustainion, given the good operation performances [79, 81, 94, 99]. Given this lack of diversity, we explored the use of PiperION AEMs for the same cell concept for the first time. The observed Faradaic efficiencies and specific energy consumptions with PiperION are comparable to the results obtained for Sustainion AEMs, making PiperION AEMs a viable alternative [60]. Furthermore, the versatility of this design is highlighted by the use of both bismuth-[79, 93, 99, 101–103] and tin-based [53, 81] catalysts, with bismuth catalysts showing greater promise. Additional operational flexibility is demonstrated through the incorporation of a gas-fed center compartment or a hydrogen oxidation-based anode [79, 94].

In terms of catalyst or materials development, certain flow cell designs may be more suitable, as they may allow for an easier implementation of reference electrodes [45, 89, 98, 104], *in operando* analysis [69, 105], and temperature or concentration control. However, DFAP holds an advantage over other reactor designs due to the absence of flooding and carbonate precipitation issues, along with the clear separation of the three compartments.[81, 106] From an application point of view, we consider DFAP to be the overall best performing and most promising reactor design for CO_2-to-HCOO(H) electroreduction. Nevertheless, CO_2-to-HCOO(H) electrolysis still encounters several challenges. Most electrolyzers rely on fluoropolymer Nafion, either as a CEM or as a binder, due to its high chemical stability, but this dependence limits their versatility [46, 47, 49, 52, 54, 55, 58–60, 62–64]. In many electrolyzers, including DFAP designs, the nucleophilic attack of hydroxide ions on the cationic moieties of AEMs may result in limited lifetimes [107]. Moreover, the anodic catalyst IrO_2 employed in DFAP is very scarce and expensive, and attempts to reduce catalyst loading may impair durability [108, 109]. Since similar problems are also encountered in the fields of proton [110, 111] and anion exchange membrane water electrolysis [112, 113], innovative developments are expected to occur rapidly, which could be adapted to the electrolysis of CO_2 to HCOO(H).

2 | Conclusion

To date, significant progress has been made in both designing and studying catalyst performance in the eCO_2RR to HCOO(H). However, despite progress, a better understanding of the reaction mechanism is still necessary. Theoretical investigations should be accompanied by *in operando* spectroscopy to detect reaction intermediates to elucidate more credible mechanistic pathways. This is not a simple task, given that different metals and operational conditions could promote different mechanisms. Besides, given the reactivity of the reaction intermediates, the design of electrolytic cells coupled with spectroscopic methods is required to identify these short-living species. Catalyst design on H-cells has centered on tin, bismuth, indium, lead, palladium, and cobalt. Among these, tin- and bismuth-based catalysts have gained popularity due to their low cost, abundance, and environmentally friendly nature. The implementation of catalysts in GDE architectures is crucial for enhancing the efficiency of the eCO_2RR and enabling the selective production of HCOOH at higher current densities. However, deactivating factors, such as electrode flooding induced by the loss of hydrophobicity or thinning of the binder, catalyst agglomeration, carbonate formation, and chemical changes, directly affect the eCO_2RR efficiency. Hence, a well-designed electrode architecture stable for long operation times is essential to guarantee constant and optimal yields. In the literature, most reported studies in flow cells utilize cathodic electrodes based on GDE with tin- and bismuth-based catalysts, along with commercial membranes. AEM-free and ZG electrolyzers primarily rely on Nafion membranes of different thicknesses (50 – 413 µm) and the use of alkaline cations in neutral or basic media (*e.g.*, $KHCO_3$, K_2SO_4, KOH) to mitigate the HER. The DFAP design typically incorporates a combination of Nafion membranes with Sustainion or PiperION AEMs to enhance the key performance parameters. While AEM-free and ZG reactor designs show promising performance, the DFAP cell has the unique advantage of producing HCOOH directly and in higher concentrations than the other reactor designs. Furthermore, the DFAP design inherently addresses challenges like flooding and salt precipitation encountered in other flow-cell designs. Hence, to achieve the required high Faradaic efficiencies and higher product concentrations over extended operation times, necessary for industrial application, this design is arguably the most promising from an industrial perspective. While currently achieved concentrations in DFAP typically fall within the range of ~13 wt%, it is worth noting that commercial HCOOH is available in concentrations ranging between 85 and 99wt%. In non-industrial processes, azeotropic distillation [52, 121] is being evaluated as a viable method to increase formic acid concentrations from 30 to 85 wt%. DFAP reactors with gas flow in the center compartment achieve more than 30 wt%, making them candidates for azeotropic distillation, however, they still require optimization for long-term operational stability. Additionally, the pervaporation [122] process to separate H_2O/HCOOH mixtures has also been proposed to obtain higher concentrations at a lower cost but is still in the research phase. Hence, future developments in these downstream processes, combined with the scaling up of the active area and cell stacking in the reactor designs, could make electrochemical formic acid production economically competitive with the current industrial methods. Industrial production of formic acid occurs on a large scale at centralized factory sites where energy consumption, including the concentration process, is optimized. Currently, the eCO_2RR to HCOOH cannot economically compete to produce concentrated HCOOH but offers a promising future in emerging applications that can utilize the diluted form. Especially direct and indirect formic acid fuel cells and biorefinery applications show optimum operation. Besides, the electrochemical production of green HCOOH is highly versatile, enabling its synthesis on a smaller scale in a decentralized manner with the possibility to couple it in a multi-synthesis reactor for post-synthetic transformations.

Acknowledgements

The authors kindly acknowledge the financial support from the German Federal Ministry of Education and Research within the project 'iNEW2.0 - Inkubator Nachhaltige Elektrochemische Wertschöpfungsketten' Project No. 03SF0627A.

26965977, 0, Downloaded from https://chemistry-europe.onlinelibrary.wiley.com/doi/10.1002/elsa.202400014 by Rwth Aachen University Universitätsbibliothek- 021000, Wiley Online Library on [10/01/2025]. See the Terms and Conditions (https://onlinelibrary.wiley.com/terms-and-conditions) on Wiley Online Library for rules of use; OA articles are governed by the applicable Creative Commons License

The authors thank Sebastian B. C. Lehmann for the contributions to graphical design.

Open access funding enabled and organized by Projekt DEAL.

Conflicts of Interest

The authors declare no conflicts of interest.

Data Availability Statement

Data sharing not applicable—no new data generated.

References

1. A. W. Zimmermann, T. Langhorst, S. Moni, J. A. Schaidle, F. Bensebaa, and A. Bardow, "Life-Cycle and Techno-Economic Assessment of Early-Stage Carbon Capture and Utilization Technologies—A Discussion of Current Challenges and Best Practices," *Frontiers in Climate* 4 (2022): 1–12.

2. O. Ellabban, H. Abu-Rub, and F. Blaabjerg, "Renewable Energy Resources: Current Status, Future Prospects and Their Enabling Technology," *Renewable and Sustainable Energy Reviews* 39 (2014): 748–764.

3. W. Zhang, Y. Hu, L. Ma, et al., "Progress and Perspective of Electrocatalytic CO_2 Reduction for Renewable Carbonaceous Fuels and Chemicals," *Advanced Science* 5 (2018): 1700275.

4. J. Hietala, A. Vuori, P. Johnsson, I. Pollari, W. Reutemann, and H. Kieczka, Formic Acid in Ullmann's Encyclopedia of Industrial Chemistry, (2016).

5. W. Zhang, Z. Jin, and Z. Chen, "Rational-Designed Principles for Electrochemical and Photoelectrochemical Upgrading of CO_2 to Value-Added Chemicals." *Advanced science* 9 (2022): 1–30.

6. P. D. Lund, J. Lindgren, J. Mikkola, and J. Salpakari, "Review of Energy System Flexibility Measures to Enable High Levels of Variable Renewable Electricity," *Renewable and Sustainable Energy Reviews* 45 (2015): 785–807.

7. A. Bhavsar, D. Hingar, S. Ostwal, I. Thakkar, S. Jadeja, and M. Shah, "The Current Scope and Stand of Carbon Capture Storage and Utilization a Comprehensive Review," *Case Studies in Chemical and Environmental Engineering* 8 (2023): 100368.

8. V. Selmert, A. Kretzschmar, H. Weinrich, H. Tempel, H. Kungl, and R. A. Eichel, "CO_2 /N_2 Separation on Highly Selective Carbon Nanofibers Investigated by Dynamic Gas Adsorption," *ChemSusChem* 15 (2022): e202200761.

9. A. Kretzschmar, V. Selmert, H. Weinrich, H. Kungl, H. Tempel, and R. A. Eichel, "Study of CO_2 Sorption Kinetics on Electrospun Polyacrylonitrile-Based Carbon Nanofibers," *Chemical Engineering & Technology* 44 (2021): 1168–1177.

10. B. Thijs, J. Rongé, and J. A. Martens, "Matching Emerging Formic Acid Synthesis Processes With Application Requirements," *Green Chemistry* 24 (2022): 2287–2295.

11. J. M. Spurgeon and B. Kumar, "A Comparative Technoeconomic Analysis of Pathways for Commercial Electrochemical CO_2 Reduction to Liquid Products," *Energy & Environmental Science* 11 (2018): 1536–1551.

12. S. M. Jordaan and C. Wang, "Electrocatalytic Conversion of Carbon Dioxide for thes Paris Goals," *Nature catalysis* 4 (2021): 915–920.

13. B. Hecker, E. Robens, H. E. Valencia, et al., "Effects of Synthesized Silver Nanoplate Structures on the Electrochemical Reduction of CO_2," *Journal of the Electrochemical Society* 170 (2023): 096505.

14. E. Robens, B. Hecker, H. Kungl, H. Tempel, and R. A. Eichel, "Bimetallic Copper–Silver Catalysts for the Electrochemical Reduction of CO_2 to Ethanol," *ACS Applied Energy Materials* 6 (2023): 7571–7577.

15. X. Zhang, S. X. Guo, K. A. Gandionco, A. M. Bond, and J. Zhang, "Electrocatalytic Carbon Dioxide Reduction: From Fundamental Principles to Catalyst Design," *Materials Today Advances* 7 (2020): 100074.

16. F. Yu, K. Deng, M. Du, W. Wang, F. Liu, and D. Liang, "Electrochemical CO_2 Reduction: From Catalysts to Reactive Thermodynamics and Kinetics," *Carbon Capture Science & Technology* 6 (2023): 100081.

17. Y. Zhang, S. X. Guo, X. Zhang, A. M. Bond, and J. Zhang, "Mechanistic Understanding of the Electrocatalytic CO_2 Reduction Reaction—New Developments Based on Advanced Instrumental Techniques," *Nano Today* 31 (2020): 100835.

18. W. Oh, C. K. Rhee, J. W. Han, and B. Shong, "Atomic and Molecular Adsorption on the Bi(111) Surface: Insights Into Catalytic CO_2 Reduction," *The Journal of Physical Chemistry C* 122 (2018): 23084–23090.

19. J. E. Pander, M. F. Baruch, and A. B. Bocarsly, "Probing the Mechanism of Aqueous CO_2 Reduction on Post-Transition-Metal Electrodes Using ATR-IR Spectroelectrochemistry," *ACS Catalysis* 6 (2016): 7824–7833.

20. J. H. Koh, D. H. Won, T. Eom, et al., "Facile CO_2 Electro-Reduction to Formate via Oxygen Bidentate Intermediate Stabilized by High-Index Planes of Bi Dendrite Catalyst," *ACS Catalysis* 7 (2017): 5071–5077.

21. Z. Sun, T. Ma, H. Tao, Q. Fan, and B. Han, "Fundamentals and Challenges of Electrochemical CO_2 Reduction Using Two-Dimensional Materials," *Chemistry* 3 (2017): 560–587.

22. I. Grigioni, L. K. Sagar, Y. C. Li, et al., "CO_2 Electroreduction to Formate at a Partial Current Density of 930 mA cm^{-2} With InP Colloidal Quantum Dot Derived Catalysts," *ACS Energy Letters* 6 (2021): 79–84.

23. S. Yang, H. An, S. Arnouts, et al., "Halide-guided Active Site Exposure in Bismuth Electrocatalysts for Selective CO_2 Conversion Into Formic Acid," *Nature catalysis* 6 (2023): 796–806.

24. M. F. Philips, D. Pavesi, T. Wissink, et al., "Electrochemical CO_2 Reduction on Gas Diffusion Electrodes: Enhanced Selectivity of In–Bi Bimetallic Particles and Catalyst Layer Optimization Through a Design of Experiment Approach," *ACS Applied Energy Materials* 5 (2022): 1720–1730.

25. C. Ye, F. Dattila, X. Chen, N. López, and M. T. M. Koper, "Influence of Cations on HCOOH and CO Formation During CO_2 Reduction on a Pd ML Pt(111) Electrode," *Journal of the American Chemical Society* 145 (2023): 19601–19610.

26. N. Han, P. Ding, L. He, Y. Li, and Y. Li, "Promises of Main Group Metal–Based Nanostructured Materials for Electrochemical CO_2 Reduction to Formate," *Advanced Energy Materials* 10 (2020): 1902338.

27. H. Zhang, Y. Ma, F. Quan, J. Huang, F. Jia, and L. Zhang, "Selective Electro-reduction of CO_2 to Formate on Nanostructured Bi From Reduction of BiOCl Nanosheets," *Electrochemistry Communications* 46 (2014): 63–66.

28. H. Weinrich, B. Rutjens, S. Basak, et al., "CO_2 Electroreduction to Formate—Comparative Study Regarding the Electrocatalytic Performance of SnO_2 Nanoparticles," *Catalysts* 13 (2023): 903.

29. S. Sen, S. M. Brown, M. L. Leonard, and F. R. Brushett, "Electroreduction of Carbon Dioxide to Formate at High Current Densities Using Tin and Tin Oxide Gas Diffusion Electrodes," *Journal of Applied Electrochemistry* 49 (2019): 917–928.

30. M. F. Baruch, J. E. Pander, J. L. White, and A. B. Bocarsly, "Mechanistic Insights Into the Reduction of CO_2 on Tin Electrodes Using in Situ ATR-IR Spectroscopy," *ACS Catalysis* 5 (2015): 3148–3156.

31. Y. Qian, Y. Liu, H. Tang, and B. L. Lin, "Highly Efficient Electroreduction of CO_2 to Formate by Nanorod@2D Nanosheets SnO," *Journal of CO2 Utilization* 42 (2020): 101287.

32. S. Zhang, P. Kang, and T. J. Meyer, "Nanostructured Tin Catalysts for Selective Electrochemical Reduction of Carbon Dioxide to Formate," *Journal of the American Chemical Society* 136 (2014): 1734–1737.

33. B. Kumar, V. Atla, J. P. Brian, et al., "Reduced SnO_2 Porous Nanowires With a High Density of Grain Boundaries as Catalysts for Efficient Electrochemical CO_2 -Into-HCOOH Conversion," *Angewandte Chemie* 129 (2017): 3699–3703.

34. S. Liu, J. Xiao, X. F. Lu, J. Wang, X. Wang, and X. W. (David) Lou, "Efficient Electrochemical Reduction of CO_2 to HCOOH Over Sub-2 Nm

26965977, 0, Downloaded from https://chemistry-europe.onlinelibrary.wiley.com/doi/10.1002/ebsa.202400014 by Rwth Aachen University Universitätsbibliothek- 021000, Wiley Online Library on [10/01/2025]. See the Terms and Conditions (https://onlinelibrary.wiley.com/terms-and-conditions) on Wiley Online Library for rules of use; OA articles are governed by the applicable Creative Commons License

SnO_2 Quantum Wires With Exposed Grain Boundaries," *Angewandte Chemie* 131 (2019): 8587–8591.

35. Z. Chen, T. Fan, Y. Q. Zhang, et al., "Wavy SnO_2 Catalyzed Simultaneous Reinforcement of Carbon Dioxide Adsorption and Activation towards Electrochemical Conversion of CO_2 to HCOOH," *Applied Catalysis B: Environment* 261 (2020): 118243.

36. S. Kim, W. J. Dong, S. Gim, et al., "Shape-controlled Bismuth Nanoflakes as Highly Selective Catalysts for Electrochemical Carbon Dioxide Reduction to Formate," *Nano Energy* 39 (2017): 44–52.

37. P. Deng, H. Wang, R. Qi, et al., "Bismuth Oxides With Enhanced Bismuth–Oxygen Structure for Efficient Electrochemical Reduction of Carbon Dioxide to Formate," *ACS Catalysis* 10 (2020): 743–750.

38. C. C. Miao and G. Q. Yuan, "Morphology-Controlled Bi_2O_3 Nanoparticles as Catalysts for Selective Electrochemical Reduction of CO_2 to Formate," *ChemElectroChem* 5 (2018): 3741–3747.

39. F. Yang, A. O. Elnabawy, R. Schimmenti, et al., "Bismuthene for Highly Efficient Carbon Dioxide Electroreduction Reaction," *Nature Communications* 11 (2020): 1088.

40. Z. Zhang, F. Ahmad, W. Zhao, et al., "Enhanced Electrocatalytic Reduction of CO_2 via Chemical Coupling Between Indium Oxide and Reduced Graphene Oxide," *Nano letters* 19 (2019): 4029–4034.

41. K. Mou, Z. Chen, S. Yao, and L. Liu, "Enhanced Electrochemical Reduction of Carbon Dioxide to Formate With in-situ Grown Indium-based Catalysts in an Aqueous Electrolyte," *Electrochimica Acta* 289 (2018): 65–71.

42. N. Zouaoui, B. D. Ossonon, M. Fan, et al., "Electroreduction of CO_2 to Formate on Amine Modified Pb Electrodes," *Journal of Materials Chemistry* 7 (2019): 11272–11281.

43. Y. Xing, M. Cui, P. Fan, et al., "Efficient and Selective Electrochemical Reduction of CO_2 to Formate on 3D Porous Structured Multi-walled Carbon Nanotubes Supported Pb Nanoparticles," *Materials Chemistry and Physics* 237 (2019): 121826.

44. A. Klinkova, P. De Luna, C. T. Dinh, et al., "Rational Design of Efficient Palladium Catalysts for Electroreduction of Carbon Dioxide to Formate," *ACS Catalysis* 6 (2016): 8115–8120.

45. J. Zou, C. Y. Lee, and G. G. Wallace *Advanced Science* 8 (2021): 1–10.

46. X. Min and M. W. Kanan, "Pd-Catalyzed Electrohydrogenation of Carbon Dioxide to Formate: High Mass Activity at Low Overpotential and Identification of the Deactivation Pathway," *Journal of the American Chemical Society* 137 (2015): 4701–4708.

47. S. Gao, X. Jiao, Z. Sun, et al., "Ultrathin Co_3O_4 Layers Realizing Optimized CO_2 Electroreduction to Formate," *Angewandte Chemie—International Edition* 55 (2016): 698–702.

48. S. Gao, Y. Lin, X. Jiao, et al., "Partially Oxidized Atomic Cobalt Layers for Carbon Dioxide Electroreduction to Liquid Fuel," *Nature* 529 (2016): 68–71.

49. S. Gao, Z. Sun, W. Liu, et al., "Atomic Layer Confined Vacancies for Atomic-level Insights Into Carbon Dioxide Electroreduction," *Nature communications* 8 (2017): 14503.

50. R. F. Weiss, "Carbon Dioxide in Water and Seawater: The Solubility of a Non-ideal Gas," *Marine Chemistry* 2 (1974): 203–215.

51. T. Burdyny and W. A. Smith, "CO_2 Reduction on Gas-diffusion Electrodes and Why Catalytic Performance Must be Assessed at Commercially-relevant Conditions," *Energy & Environmental Science* 12 (2019): 1442–1453.

52. M. Jouny, W. Luc, and F. Jiao, "General Techno-Economic Analysis of CO_2 Electrolysis Systems," *Industrial & Engineering Chemistry Research* 57 (2018): 2165–2177.

53. V. Theußl, H. Weinrich, C. Heume, et al., "Impact of the Carbon Substrate for Gas Diffusion Electrodes on the Electroreduction of CO_2 to Formate," *ChemElectroChem* 10 (2023): e202300121.

54. K. Yang, R. Kas, W. A. Smith, and T. Burdyny, "Role of the Carbon-Based Gas Diffusion Layer on Flooding in a Gas Diffusion Electrode Cell for Electrochemical CO_2 Reduction," *ACS Energy Letters* 6 (2021): 33–40.

55. A. A. Samu, I. Szenti, Á. Kukovecz, B. Endrődi, and C. Janáky, "Systematic Screening of Gas Diffusion Layers for High Performance CO_2 Electrolysis," *Communications Chemistry* 6 (2023): 1–9.

56. C. Martens, B. Schmid, H. Tempel, and R. A. Eichel, "CO_2 Flow Electrolysis—limiting Impact of Heat and Gas Evolution in the Electrolyte Gap on Current Density," *Green Chemistry* 25 (2023): 7794–7806.

57. N. Hussain, E. Van Steen, S. Tanaka, and P. Levecque, "Metal Based Gas Diffusion Layers for Enhanced Fuel Cell Performance at High Current Densities," *Journal of Power Sources* 337 (2017): 18–24.

58. C. T. Dinh, T. Burdyny, G. Kibria, et al., "CO_2 Electroreduction to Ethylene via Hydroxide-mediated Copper Catalysis at an Abrupt Interface," *Science* 360 (2018): 783–787.

59. V. Theußl, H. Weinrich, F. Lisi, H. Tempel, and R.-A. Eichel, "Early-stage Performance Change of Gas Diffusion Electrodes for CO_2 Electroreduction to Formate," *Sustainable Energy & Fuels* 8 (2024): 1483–1494.

60. B. Rutjens, K. von Foerster, B. Schmid, et al., "Impact of the PiperION Anoin Exchange Membrane Thickness on the Performance of a CO_2-to- HCOOH Three- Compartment Electrolyzer." *Industrial & Engineering Chemistry Research* 63 (2024): 3986–3996.

61. M. F. Philips, G.-J. M. Gruter, M. T. M. Koper, and K. J. P. Schouten, "Optimizing the Electrochemical Reduction of CO_2 to Formate: A State-of-the-Art Analysis," *ACS Sustainable Chemistry & Engineering* 8 (2020): 15430–15444.

62. F. Bienen, A. Löwe, J. Hildebrand, et al., "Degradation Study on Tin- and Bismuth-based Gas-diffusion Electrodes During Electrochemical CO_2 Reduction in Highly Alkaline media," *The Journal of Energy Chemistry* 62 (2021): 367–376.

63. K. Van Daele, B. De Mot, M. Pupo, et al., "Sn-Based Electrocatalyst Stability: A Crucial Piece to the Puzzle for the Electrochemical CO_2 Reduction Toward Formic Acid," *ACS Energy Letters* 6 (2021): 4317–4327.

64. Y. Kong, M. Liu, H. Hu, et al., "Cracks as Efficient Tools to Mitigate Flooding in Gas Diffusion Electrodes Used for the Electrochemical Reduction of Carbon Dioxide," *Small Methods* 6 (2022): 2200369.

65. M. E. Leonard, M. J. Orella, N. Aiello, Y. Román-Leshkov, A. Forner-Cuenca, and F. R. Brushett, "Editors' Choice—Flooded by Success: On the Role of Electrode Wettability in CO_2 Electrolyzers That Generate Liquid Products," *Journal of the Electrochemical Society* 167 (2020): 124521.

66. A. M. Kalde, M. Grosseheide, S. Brosch, et al., "Micromodel of a Gas Diffusion Electrode Tracks in-Operando Pore-Scale Wetting Phenomena," *Small* 18 (2022): 2204012.

67. S. Brosch, F. Wiesner, A. Decker, J. Linkhorst, and M. Wessling, "Spatio-Temporal Electrowetting and Reaction Monitoring in Microfluidic Gas Diffusion Electrode Elucidates Mass Transport Limitations," *Small* 20 (2024): 2310427.

68. U. O. Nwabara, A. D. Hernandez, D. A. Henckel, et al., "Binder-Focused Approaches to Improve the Stability of Cathodes for CO_2 Electroreduction," *ACS Applied Energy Materials* 4 (2021): 5175–5186.

69. A. B. Moss, S. Garg, M. Mirolo, et al., "In Operando Investigations of Oscillatory Water and Carbonate Effects in MEA-based CO_2 Electrolysis Devices," *Joule* 7 (2023): 350–365.

70. E. R. Cofell, U. O. Nwabara, S. S. Bhargava, D. E. Henckel, and P. J. A. Kenis, "Investigation of Electrolyte-Dependent Carbonate Formation on Gas Diffusion Electrodes for CO_2 Electrolysis," *ACS Applied Materials & Interfaces* 13 (2021): 15132–15142.

71. U. O. Nwabara, E. R. Cofell, S. Verma, E. Negro, and P. J. A. Kenis, "Durable Cathodes and Electrolyzers for the Efficient Aqueous Electrochemical Reduction of CO_2," *ChemSusChem* 13 (2020): 855–875.

26985977, 0, Downloaded from https://chemistry-europe.onlinelibrary.wiley.com/doi/10.1002/elsa.202400014 by Rwth Aachen University Universitätsbibliothek- 021000, Wiley Online Library on [10/01/2025]. See the Terms and Conditions (https://onlinelibrary.wiley.com/terms-and-conditions) on Wiley Online Library for rules of use; OA articles are governed by the applicable Creative Commons License

72. R. V. Mom, L. E. Sandoval-Diaz, D. Gao, et al., "Assessment of the Degradation Mechanisms of Cu Electrodes During the CO_2 Reduction Reaction," *ACS Applied Materials & Interfaces* 15 (2023): 30052–30059.

73. Y. Wu, S. Garg, M. Li, et al., "Effects of Microporous Layer on Electrolyte Flooding in Gas Diffusion Electrodes and Selectivity of CO_2 Electrolysis to CO," *Journal of Power Sources* 522 (2022): 230998.

74. B. Kim, F. Hillman, M. Ariyoshi, S. Fujikawa, and P. J. A. Kenis, "Effects of Composition of the Micro Porous Layer and the Substrate on Performance in the Electrochemical Reduction of CO_2 to CO," *Journal of Power Sources* 312 (2016): 192–198.

75. N. T. Nesbitt, T. Burdyny, H. Simonson, et al., "Liquid–Solid Boundaries Dominate Activity of CO_2 Reduction on Gas-Diffusion Electrodes," *ACS Catalysis* 10 (2020): 14093–14106.

76. G. Lin and T. Van Nguyen, "Effect of Thickness and Hydrophobic Polymer Content of the Gas Diffusion Layer on Electrode Flooding Level in a PEMFC," *Journal of the Electrochemical Society* 152 (2005): A1942.

77. Q. Chen, A. Kube, D. Schonvogel, D. Kopljar, E. Klemm, and K. A. Friedrich, "Elucidating Key Mechanistic Processes During Acidic CO_2 Electroreduction on Gas Diffusion Electrodes towards Stable Production of Formic Acid," *Chemical Engineering Journal* 476 (2023): 146486.

78. C. Ampelli, F. Tavella, D. Giusi, A. M. Ronsisvalle, S. Perathoner, and G. Centi, "Electrode and Cell Design for CO_2 Reduction: A Viewpoint," *Catalysis Today* 421 (2023): 114217.

79. L. Fan, C. Xia, P. Zhu, Y. Lu, and H. Wang, "Electrochemical CO_2 reduction to high-concentration pure formic acid solutions in an all-solid-state reactor." *Nature Communications* 11 (2020): 1–9.

80. Y. Wang, L. Xu, L. Zhan, et al., "Electron Accumulation Enables Bi Efficient CO_2 Reduction for Formate Production to Boost Clean Zn-CO_2 Batteries," *Nano Energy* 92 (2022): 106780.

81. H. Yang, J. J. Kaczur, S. D. Sajjad, and R. I. Masel, "Electrochemical Conversion of CO_2 to Formic Acid Utilizing Sustainion™ Membranes," *Journal of CO2 Utilization* 20 (2017): 208–217.

82. M. Quentmeier, B. Schmid, H. Tempel, and R. A. Eichel, "Modular CO_2 -to-CO Electrolysis Short-Stack Design—Impact of Temperature Gradients and Insights Into Position-Dependent Cell Behavior," *ACS Sustainable Chemistry & Engineering* 12 (2024): 3876–3885.

83. M. Quentmeier, B. Schmid, H. Tempel, H. Kungl, and R. A. Eichel, "Toward a Stackable CO_2 -to-CO Electrolyzer Cell Design—Impact of Media Flow Optimization," *ACS Sustainable Chemistry & Engineering* 11 (2023): 679–688.

84. L. C. Brée, M. Wessling, and A. Mitsos, "Modular Modeling of Electrochemical Reactors: Comparison of CO_2-electolyzers," *Computers & Chemical Engineering* 139 (2020): 106890.

85. J. B. Vennekoetter, R. Sengpiel, and M. Wessling, "Beyond the Catalyst: How Electrode and Reactor Design Determine the Product Spectrum During Electrochemical CO_2 Reduction," *Chemical Engineering Journal* 364 (2019): 89–101.

86. P. Ding, J. Zhang, N. Han, Y. Zhou, L. Jia, and Y. Li, "Simultaneous Power Generation and CO_2 Valorization by Aqueous Al–CO_2 Batteries Using Nanostructured Bi 2 S 3 as the Cathode Electrocatalyst," *Journal of Materials Chemistry* 8 (2020): 12385–12390.

87. T. Reichbauer, B. Schmid, K. M. Vetter, et al., "Electrical Energy Input Efficiency Limitations in CO_2 -to-CO Electrolysis and Attempts for Improvement," *Electrochemical Science Advances* 00 (2023): e2300024.

88. C. W. Lee, J. S. Hong, K. D. Yang, et al., "Selective Electrochemical Production of Formate From Carbon Dioxide With Bismuth-Based Catalysts in an Aqueous Electrolyte," *ACS Catalysis* 8 (2018): 931–937.

89. J. Baessler, T. Oliveira, R. Keller, and M. Wessling, "Paired Electrosynthesis of Formic Acid From CO_2 and Formaldehyde From Methanol," *ACS Sustainable Chemistry & Engineering* 11 (2023): 6822–6828.

90. L. Hu, J. A. Wrubel, C. M. Baez-Cotto, et al., "A Scalable Membrane Electrode Assembly Architecture for Efficient Electrochemical Conversion of CO_2 to Formic Acid," *Nature communications* 14 (2023): 7605.

91. A. Löwe, M. Schmidt, F. Bienen, D. Kopljar, N. Wagner, and E. Klemm, "Optimizing Reaction Conditions and Gas Diffusion Electrodes Applied in the CO_2 Reduction Reaction to Formate to Reach Current Densities up to 1.8 A cm^{-2}," *ACS Sustainable Chemistry & Engineering* 9 (2021): 4213–4223.

92. I. Montiel, A. Dutta, K. Kiran, et al., "CO_2 Conversion at High Current Densities: Stabilization of Bi(III)-Containing Electrocatalysts Under CO_2 Gas Flow Conditions," *ACS Catalysis* 12 (2022): 10872–10886.

93. T. Fan, W. Ma, M. Xie, et al., "Achieving High Current Density for Electrocatalytic Reduction of CO_2 to Formate on Bismuth-based Catalysts," *Cell Reports Physical Science* 2 (2021): 100353.

94. C. Xia, P. Zhu, Q. Jiang, et al., "Continuous Production of Pure Liquid Fuel Solutions via Electrocatalytic CO_2 Reduction Using Solid-electrolyte Devices," *Nature Energy* 4 (2019): 776–785.

95. X. Guo, S. M. Xu, H. Zhou, et al., "Engineering Hydrogen Generation Sites to Promote Electrocatalytic CO_2 Reduction to Formate," *ACS Catalysis* 12 (2022): 10551–10559.

96. M. Ramdin, A. R. T. Morrison, M. De Groen, et al., "High-Pressure Electrochemical Reduction of CO_2 to Formic Acid/Formate: Effect of pH on the Downstream Separation Process and Economics," *Industrial & Engineering Chemistry Research* 58 (2019): 22718–22740.

97. X. Wu, Y. Zhang, Y. Yang, et al., "Ni2P With Phosphorus Vacancy Supported Pt Clusters for Efficiently Electrocatalytic co-production of Hydrogen and Value-added Chemicals From Methanol-water at Low Potential," *Chemical Engineering Journal* 452 (2023): 139057.

98. L. Li, Z. Liu, X. Yu, and M. Zhong, "Achieving High Single-Pass Carbon Conversion Efficiencies in Durable CO_2 Electroreduction in Strong Acids via Electrode Structure Engineering," *Angewandte Chemie* 135 (2023): e202300226.

99. H. Yang, J. J. Kaczur, S. D. Sajjad, and R. I. Masel, "Performance and Long-term Stability of CO_2 Conversion to Formic Acid Using a Three-compartment Electrolyzer Design," *Journal of CO2 Utilization* 42 (2020): 101349.

100. T. Yan, H. Pan, Z. Liu, and P. Kang, "Phase-Inversion Induced 3D Electrode for Direct Acidic Electroreduction CO_2 to Formic Acid," *Small* 19 (2023): 2207650.

101. J. Zeng, P. Jagdale, M. A. O. Lourenço, et al., "Biochar-Supported BiOx for Effective Electrosynthesis of Formic Acid From Carbon Dioxide Reduction," *Crystals* 11 (2021): 363.

102. Y. Wang, C. Wang, Y. Wei, et al., "Efficient and Selective Electroreduction of CO_2 to HCOOH over Bismuth-Based Bromide Perovskites in Acidic Electrolytes," *Chemistry – A European Journal* 28 (2022): e20221832.

103. S. Van Daele, L. Hintjens, S. Hoekx, et al., "How Flue Gas Impurities Affect the Electrochemical Reduction of CO_2 to CO and Formate," *Applied Catalysis B: Environment and Energy* 341 (2024): 123345.

104. H. P. Iglesias van Montfort, S. Subramanian, E. Irtem, et al., "An Advanced Guide to Assembly and Operation of CO_2 Electrolyzers," *ACS Energy Letters* 8 (2023): 4156–4161.

105. S. Chang, Y. Xuan, Q. Wang, and K. Wang, "Bimetallic in–Sn Core–Shell Catalyst Enabling Highly Efficient Electrocatalytic CO_2 Reduction to Formate," *ACS Applied Energy Materials* 1 (2023): 1514–1523.

106. A. Kaur, B. Kim, R. Dinsdale, A. Guwy, E. Yu, and G. Premier, "Challenges in Scale-up of Electrochemical CO_2 Reduction to Formate Integrated With Product Extraction Using Electrodialysis," *Journal of Chemical Technology & Biotechnology* 96 (2021): 2461–2471.

107. G. Merle, M. Wessling, and K. Nijmeijer, "Anion Exchange Membranes for Alkaline Fuel Cells: A Review," *Journal of Membrane Science* 377 (2011): 1–35.

108. K. M. Vetter, C. Aring da Silva Ramos Mauro, D. Reinisch, et al., "Stability Evaluation of Earth-Abundant Metal-Based Polyoxometalate

26965977, 0, Downloaded from https://chemistry-europe.onlinelibrary.wiley.com/doi/10.1002/ebsa.202400014 by Rwth Aachen University Universitätsbibliothek- 021000, Wiley Online Library on [10/01/2025]. See the Terms and Conditions (https://onlinelibrary.wiley.com/terms-and-conditions) on Wiley Online Library for rules of use; OA articles are governed by the applicable Creative Commons License

Electrocatalysts for Oxygen Evolution Reaction towards Industrial PEM Electrolysis at High Current Densities," *Electrochemical Science Advances* 2 (2022): e202100073.

109. F. Hegge, F. Lombeck, E. Cruz Ortiz, et al., "Efficient and Stable Low Iridium Loaded Anodes for PEM Water Electrolysis Made Possible by Nanofiber Interlayers," *ACS Applied Energy Materials* 3 (2020): 8276–8284.

110. Z. Y. Wu, F. Y. Chen, B. Li, et al., "Non-iridium-based Electrocatalyst for Durable Acidic Oxygen Evolution Reaction in Proton Exchange Membrane Water Electrolysis," *Nature Materials* 22 (2023): 100–108.

111. M. Di Virgilio, A. Basso Peressut, V. Arosio, A. Arrigoni, S. Latorrata, and G. Dotelli, "Functional and Environmental Performances of Novel Electrolytic Membranes for PEM Fuel Cells: A Lab-Scale Case Study," *Clean Technologies* 5 (2023): 74–93.

112. N. Chen, S. Y. Paek, J. Y. Lee, J. H. Park, S. Y. Lee, and Y. M. Lee, "High-performance Anion Exchange Membrane Water Electrolyzers With a Current Density of 7.68 A cm −2 and a Durability of 1000 Hours," *Energy & Environmental Science* 14 (2021): 6338–6348.

113. R. Vinodh, S. S. Kalanur, S. K. Natarajan, and B. G. Pollet, "Recent Advancements of Polymeric Membranes in Anion Exchange Membrane Water Electrolyzer (AEMWE): A Critical Review," *Polymers* 15 (2023): 2144.

114. Z. Wang, Y. Zhou, C. Xia, W. Guo, B. You, and B. Y. Xia, "Efficient Electroconversion of Carbon Dioxide to Formate by a Reconstructed Amino-Functionalized Indium–Organic Framework Electrocatalyst," *Angewandte Chemie—International Edtion* 60 (2021): 19107–19112.

115. B. De Mot, M. Ramdin, J. Hereijgers, T. J. H. Vlugt, and T. Breugelmans, "Direct Water Injection in Catholyte-Free Zero-Gap Carbon Dioxide Electrolyzers," *ChemElectroChem* 7 (2020): 3839–3843.

116. W. Lee, Y. E. Kim, M. H. Youn, S. K. Jeong, and K. T. Park, "Catholyte-Free Electrocatalytic CO_2 Reduction to Formate," *Angewandte Chemie—International Edition* 57 (2018): 6883–6887.

117. J. Li, J. Jiao, H. Zhang, et al., "Two-Dimensional SnO_2 Nanosheets for Efficient Carbon Dioxide Electroreduction to Formate," *ACS Sustainable Chemistry & Engineering* 8 (2020): 4975–4982.

118. Y. Kong, L. Wang, H. Jiang, et al., "Design of Counter Oxidation vs. CO_2 Electroreduction for Efficient Formate Production on a Tin Cathode," *J Electroanal Chem* 847 (2019): 113264.

119. G. Díaz-Sainz, M. Alvarez-Guerra, B. Ávila-Bolívar, J. Solla-Gullón, V. Montiel, and A. Irabien, "Improving Trade-offs in the Figures of Merit of Gas-phase Single-pass Continuous CO_2 Electrocatalytic Reduction to Formate," *Chemical Engineering Journal* 405 (2021): 126965.

120. Z. Tan, J. Zhang, Y. Yang, et al., "Continuous Production of Formic Acid Solution From Electrocatalytic CO_2 Reduction Using Mesoporous Bi_2O_3 Nanosheets as Catalyst," *CCS Chem* 6 (2023): 100–109.

121. F. Proietto, A. Galia, and O. Scialdone, "Towards the Electrochemical Conversion of CO_2 to Formic Acid at an Applicative Scale: Technical and Economic Analysis of Most Promising Routes," *ChemElectroChem* 8 (2021): 2169–2179.

122. J. J. Kaczur, L. J. McGlaughlin, and P. S. Lakkaraju, "Investigating Pervaporation as a Process Method for Concentrating Formic Acid Produced from Carbon Dioxide," *Journal of Carbon Research* 6 (2020): 42.

26985977, 0, Downloaded from https://chemistry-europe.onlinelibrary.wiley.com/doi/10.1002/elsa.202400014 by Rwth Aachen University Universitätsbibliothek- 021000, Wiley Online Library on [10/01/2025]. See the Terms and Conditions (https://onlinelibrary.wiley.com/terms-and-conditions) on Wiley Online Library for rules of use; OA articles are governed by the applicable Creative Commons License